Int. J. Heat Mass Transfer. Vol. 29, No. 8, pp. 1245–1251, 1986
Printed in Great Britain

0017–9310/86 $3.00+0.00
Pergamon Journals Ltd.

Post-dryout heat transfer to Freon in a vertical tube at high subcritical pressures

KANEYASU NISHIKAWA,* SUGURU YOSHIDA, HIDEO MORI and HIROSHI TAKAMATSU†

Department of Mechanical Engineering, Faculty of Engineering, Kyushu University, 10-1, Hakozaki 6-chome, Higashi-ku, Fukuoka, 812 Japan

Abstract—Studies of the post-dryout heat transfer were made based on experimental data of the heat transfer to Freon 22 flowing upward in a vertical, round tube at high subcritical pressures (reduced pressures of 0.68–0.92). A conventional theoretical model failed in part to reproduce the measured wall temperature. A nondimensional parameter *Kn* was introduced to a model for the post-dryout regime to take account of the thermodynamic nonequilibrium between the vapor and the liquid droplets. A correlation of *Kn* was developed and a method using this correlation was successful in predicting the wall temperature.

1. INTRODUCTION

In the design of a once-through type of vapor generator, knowledge is required of the critical heat flux and the heat transfer coefficient or wall temperature in the regime beyond the critical heat flux for boiling liquid in a tube. The present authors have been investigating these subjects in relation to the safety and high performance of a vapor generator in a power plant, in particular using Freon at high subcritical pressure as its working fluid. Empirical correlations were developed of the critical heat flux or the critical quality [1, 2]. Furthermore, in the post-dryout heat transfer (this term will be used in the present paper to denote the heat transfer beyond the critical heat flux at relatively high quality), two typical distributions of the wall temperature were observed depending on the mass velocity, and these different wall temperature distributions were found to be due to the distinctive behavior of the actual quality in thermodynamic nonequilibrium of the vapor–liquid mixture in the post-dryout region [3].

The purpose of the present paper is to obtain further data of the post-dryout heat transfer to Freon at high subcritical pressures in addition to the previous experiment, and to develop a method of predicting the post-dryout heat transfer.

2. EXPERIMENTAL APPARATUS AND PROCEDURE

The experimental apparatus and procedure are the same as described in the previous paper [3], except the inside diameter of the test section.

The test section was an AISI 316 stainless-steel round tube of 12 mm O.D. and 9 mm I.D., heated over a 2-m length by passing alternating current directly through the tubing. The fluid flows vertically upward in the tube. The fluid temperatures were measured at the inlet and outlet mixing chambers and the pressure was measured at the inlet. The inside surface temperatures were evaluated from outside surface temperatures measured with 19 thermocouples welded on the outside surface at regular longitudinal intervals of 100 mm.

Freon 22 was used as the test fluid, and the previous experimental conditions were extended in the present experiment to the following ranges of parameters

pressure: 3.4 $\sim$ 4.6 MPa
(reduced pressure: 0.68 $\sim$ 0.92)
mass velocity: 400 $\sim$ 1600 kg m^{-2} s^{-1}
surface heat flux: 12 $\sim$ 70 kW m^{-2}.

In the following analyses, use will be made of the previous data for a 13-mm-I.D. tube [3] as well as the present data.

3. EXPERIMENTAL RESULTS

Figures 1 and 2 show the typical examples of the inside surface temperatures plotted against the bulk fluid enthalpy at high and low mass velocities, respectively. The data of several experimental runs with different inlet enthalpies are shown with different symbols. A distribution of the wall temperature which would be realized along a sufficiently long tube might be estimated from these data as described previously [3]. The arrow in each figure indicates the point of the critical quality predicted from the correlations [1, 2]. For both the examples, the critical heat flux conditions belong to Regime 1 reported in the previous paper [1], in which the critical quality is relatively high. While the wall temperature, after an abrupt rise to the maximum, declines gradually with an increase of fluid enthalpy at a high mass velocity as shown in Fig. 1, the wall temperature continues to rise gradually with

* Present address: Kurume College of Technology, 1232 Komorino, Kurume, 830 Japan.

† Present address: Research Institute of Industrial Science, Kyushu University, 33 Kasuga, Sakamoto, Kasuga, 816 Japan.

NOMENCLATURE

A_d total surface area of the liquid droplets per unit area of the inside surface of the tube
C_D drag coefficient
c_p specific heat at constant pressure
D inside diameter of the tube
D_d droplet diameter
G mass velocity
g acceleration due to gravity
h specific enthalpy
h_{fg} latent heat of vaporization
Kn nondimensional parameter to take account of thermodynamic nonequilibrium, defined by equation (9)
L distance from the point of dryout
N number of the liquid droplets per unit volume
P pressure
Pr Prandtl number
q heat flux on the inside surface of the tube
q_d heat transfer rate to the liquid droplets per unit area of the inside surface of the tube
S slip ratio
T temperature
T_s saturated temperature
T_w inside surface temperature of the tube
u velocity
x vapor mass fraction in the thermodynamic equilibrium state, $0 \leqslant x \leqslant 1$
x_a actual quality
x_e thermodynamic equilibrium quality defined by $(h_b - h_l)/h_{fg}$, also extended to the superheated vapor region.

Greek symbols
α heat transfer coefficient from the tube wall to the bulk vapor, defined by equation (2)
α_d heat transfer coefficient from the bulk vapor to the liquid droplet
λ thermal conductivity
μ viscosity
ρ density
σ surface tension.

Subscripts
b bulk fluid
c dryout point
d liquid droplet
l saturated liquid
v vapor
vs dry saturated vapor.

increasing fluid enthalpy after the initial rapid rise at the lower mass velocity as shown in Fig. 2. The same tendency was observed in the previous experiment [3] with a 13-mm-I.D. tube, and no significant difference was recognized between the measured wall temperatures of 9- and 13-mm-I.D. tubes.

Several correlations [4–7] have been proposed for a post-dryout heat transfer mainly to water. The values estimated from these correlations are also shown in Figs. 1 and 2. As pointed out previously [3], neither correlation by Groeneveld and Delorme [4] nor by Plummer *et al.* [5] predicts such an effect of mass velocity on the wall temperature as indicated by the measurements. Two correlations by Saha [6] are successful in predicting the wall temperatures at the low mass velocity, but less successful at the higher mass

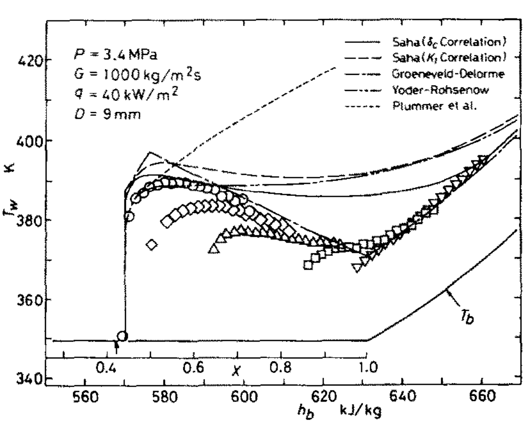

FIG. 1. Measured and predicted wall temperature distributions.

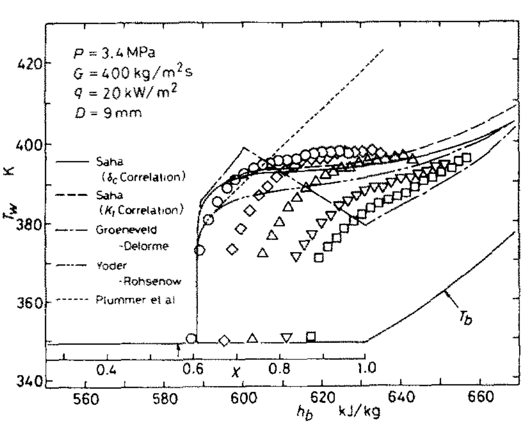

FIG. 2. Measured and predicted wall temperature distributions.

velocity. Besides, Saha's correlations were found, though no example is shown, to have a tendency to overestimate the wall temperature with increase of pressure. The wall temperatures by Yoder and Rohsenow's correlation [7] are slightly below the measured values at low mass velocity, the difference being larger with increase of pressure, and the agreement is not good at the high mass velocity, especially in the region of high quality. None of the correlations thus predict satisfactorily such an effect of mass velocity as described above.

4. THEORETICAL ANALYSIS

In the present study, the region of quality higher than 0.4 will be considered. The first abrupt rise of the wall temperature in such a quality region is caused mainly by the critical heat flux condition which belongs to Regime 1 according to the authors' classification [1]. This critical heat flux condition is supposed to correspond to the dryout of the thin liquid film on the wall surface and in the post-dryout region the dispersed liquid droplets are assumed to flow in the continuous vapor medium.

As described in ref. [3], the heat is supposed to be transferred to Freon in the post-dryout region at such high quality as mentioned above by two paths: convective heat transfer from the wall to the bulk vapor and convective heat transfer from the bulk vapor to the liquid droplets entrained in the vapor, because the radiative heat transfer is negligibly small—at least in the case of Freon—and because the contribution of heat transfer direct from the wall to the liquid droplets is considered to be small except in the low quality region.

A correlation of the single-phase heat transfer to superheated vapor of Freon was developed in ref. [3]. This correlation was slightly modified based on the present data. Assuming this modified correlation can be applied to the convective heat transfer from the wall to the vapor in the post-dryout region, the correlation is written as follows

$$\frac{\alpha D}{\lambda_v} = 0.0048\left\{\left(\frac{GD}{\mu_v}\right)\left[x_a + \frac{\rho_v}{\rho_l}(1-x_a)\right]\right\}^{0.92} \times Pr_v^{0.4}\left[1 + \frac{2.0}{(L/D)^{1.1}}\right] \quad (1)$$

where the heat transfer coefficient α is defined as

$$\alpha = \frac{q}{T_w - T_v}. \quad (2)$$

The actual quality x_a in equation (1) is related to the actual enthalpy of the vapor h_v and the bulk fluid enthalpy h_b, or the thermodynamic equilibrium quality x_e as

$$x_a = \frac{h_b - h_l}{h_v - h_l} = \frac{h_{fg}}{h_v - h_l}x_e. \quad (3)$$

The actual quality x_a is not equal to the thermodynamic equilibrium quality x_e because of the thermodynamic nonequilibrium between the vapor and the liquid droplets. If the value of the actual quality is known, the wall temperature can be predicted by equations (1)–(3) for the prescribed heat flux.

For the post-dryout heat transfer, several theoretical analyses have been developed [8–10], based on the models formulating each of the constituent elementary processes. Referring to these analyses, which were not especially intended for such high subcritical pressures as are used in the present study, an attempt was made to estimate the actual quality based on a model shown in the Appendix and consequently the wall temperature by equations (1)–(3).

The wall temperature T_w and the actual quality x_a thus calculated are plotted against the equilibrium quality x_e at a low mass velocity in Fig. 3. The experimental wall temperature and the actual quality are also shown in this figure. The experimental value of the actual quality was obtained by the iterative calculation using equations (1)–(3) to satisfy the measured wall temperature, since no direct measurement of the actual quality, which was quite difficult under the present experimental conditions, was made. The actual quality and the wall temperature calculated from the present analysis were found to depend strongly upon the liquid droplet diameter D_{dc} at the dryout point, which is one of the boundary conditions for the system of equations, but depended only slightly upon the droplet velocity u_{dc} or slip ratio $S_c = u_{vc}/u_{dc}$ at the dryout point. Both the wall temperatures, shown by the broken line and the dot-dash line in

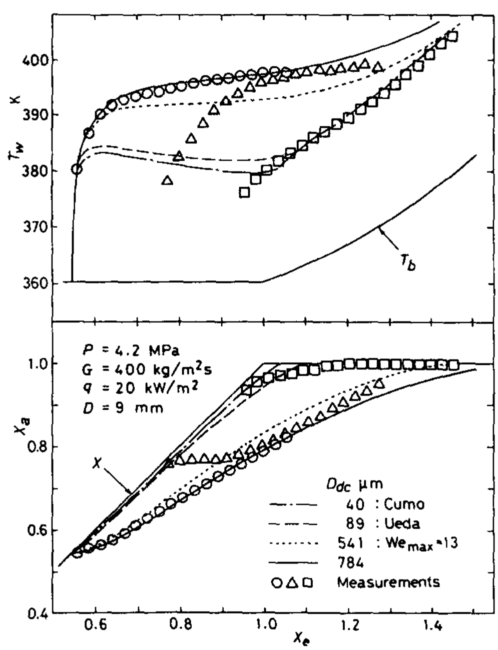

FIG. 3. Calculated and measured wall temperature and actual quality vs equilibrium quality.

the figure, calculated with the dryout-point droplet diameter by Ueda's correlation [11] and Cumo's [12], respectively, are considerably lower than the measured values. This is due to the larger values of the actual quality, that is, the predicted actual qualities being little different from the equilibrium vapor mass fraction x, because of the underestimation of the size of the liquid droplets. The solid line in the figure shows the results calculated by choosing the value of the dryout-point droplet diameter so that the wall temperature was fitted with the measured values as well as possible. Indeed these results agree very well with the experimental values, but, in this case, the dryout-point droplet diameter is 0.78 mm and the maximum value of the Weber number, $We = \rho_v(u_v - u_d)^2 D_d/\sigma$, is 29. This value of the maximum Weber number is considerably larger than the critical Weber number, the value of which is, in general, found to be around 13 for a liquid droplet entrained in the gas-phase flow. The maximum Weber number at which the best-fitted wall temperature was calculated became larger with increase of pressure and was 55 at a pressure of 4.6 MPa. Taking this into account, the calculation was carried out under the limitation of the Weber number being always less than the critical value of 13. This result is shown by the dotted line. The calculated wall temperatures are somewhat lower than the measured values and the difference between them was found to be more marked with increase of pressure.

It was found by a similar comparison of the analysis with the measurement at the higher mass velocity that the analysis did not predict satisfactorily the remarkable tendency of the wall temperature which reduces with increase of bulk fluid enthalpy, though the maximum Weber number in this case remained below the critical value.

5. PREDICTION METHOD OF ACTUAL QUALITY AND WALL TEMPERATURE

The theoretical calculations in the preceding section were not completely successful in reproducing the measured wall temperature. The reasons are supposed to be that each elementary process might not be modeled with entire propriety, and/or that other factors might yet remain to be taken into account. Since it was, however, difficult to give further detailed considerations to these problems, the following analysis was made.

From the energy equation for the two-phase flow in the post-dryout region, the following relation is obtained

$$\frac{\mathrm{d}x_a}{\mathrm{d}x_e} = \frac{q_d}{q} \tag{4}$$

where

$$q_d = \alpha_d A_d (T_v - T_s). \tag{5}$$

Equation (3) is rewritten as

$$T_v - T_s = \frac{h_v - h_{vs}}{c_{pv}} = \frac{h_{fg}}{c_{pv}}\left(\frac{x_e}{x_a} - 1\right). \tag{6}$$

Substitution of equations (5) and (6) into equation (4) yields

$$\frac{\mathrm{d}x_a}{\mathrm{d}x_e} = \frac{1}{Bo Kn}\left(\frac{x_e}{x_a} - 1\right) \tag{7}$$

where

$$Bo = \frac{q}{G h_{fg}} \tag{8}$$

and

$$Kn = \frac{G c_{pv}}{\alpha_d A_d}. \tag{9}$$

The actual quality can be estimated by solving equation (7) with the boundary condition:

$$x_a = x_c \quad \text{at} \quad x_e = x_c. \tag{10}$$

The coefficient in equation (7) consists of two nondimensional parameters, Bo and Kn. Bo is the so-called boiling number and represents the change of the vapor mass fraction per unit tube length at thermodynamic equilibrium; hence the higher value of the boiling number means the stronger acceleration of the two-phase flow in the post-dryout region. The nondimensional parameter Kn represents the ratio of the heat capacitance of the vapor flow to the thermal conductance from the vapor to the liquid droplets; therefore the parameter Kn is considered to be a characteristic parameter which governs the thermodynamic nonequilibrium of the dispersed two-phase flow. As Kn increases, the two-phase fluid departs farther from the thermodynamic equilibrium state.

On reference to the theoretical analysis in the preceding section, the parameter Kn was supposed to be described as a function of following nondimensional parameters:

$$Kn = f\left(\frac{GD}{\mu_v}, \frac{G^2 D}{\sigma\rho_v}, \frac{\rho_v(\rho_l - \rho_v)gD}{G^2}, \frac{q}{G h_{fg}}, Pr_v, \frac{\rho_v}{\rho_l}, \frac{\rho_l}{\rho_v} - 1, x_a, 1 - x_a, \frac{x_e}{x_a} - 1, x_c\right). \tag{11}$$

Based on the present and previous [3] experimental data, the following correlation of Kn was obtained.

$$Kn = 4.26 \times 10^3 \left(\frac{GD}{\mu_v}\right)^{0.52} \left(\frac{G^2 D}{\sigma\rho_v}\right)^{-0.73} Pr_v^{0.3} \left(\frac{\rho_v}{\rho_l}\right)^{0.3} x_a^n \times (1 - x_a)^{-0.20} \left(\frac{x_e}{x_a} - 1\right)^{0.83} \tag{12}$$

where

$$n = 2.0 \exp\left[-1.3\left(\frac{G\mu_v}{\sigma\rho_v}\right)\left(\frac{\rho_l}{\rho_v} - 1\right)^{1.7}\right] - 1. \tag{13}$$

The actual quality was estimated by solving equation (7) numerically together with equation (12), and by the use of this actual quality value the wall temperature was calculated from equations (1)–(3) for a given pressure, mass velocity and wall heat flux.

Figures 4 and 5 show the examples of the comparison of the wall temperature and the actual quality calculated by this method with the measured values. The circle marks indicate the data in such a case as the rapid wall temperature rise occurs near the critical quality predicted by the correlation [1, 2], this quality being shown by an arrow, while the triangle and square marks are the cases of the quality at the tube inlet above the predicted critical quality. The calculated values corresponding to the former and latter cases are shown with solid and broken lines, respectively. Although a somewhat large difference is noted between the calculated and measured values shown by triangle marks, the calculations agree well in general with the measurements.

Figure 6 shows the comparison of the predictions and measurements under the various conditions in terms of the difference between the wall temperature and the bulk fluid temperature (the saturated temperature in the saturated region). It should be noted that almost all data points lie within $\pm 20\%$.

No experimental data have apparently been published to date of the post-dryout heat transfer to Freon at such high pressures as in the present study. Data were obtained by Groeneveld [13] and Schnittger [14] for Freon 12 at rather low pressures. Figure 7 shows the examples of the comparison of their data with the predicted wall temperatures. The present method is successful also in these cases.

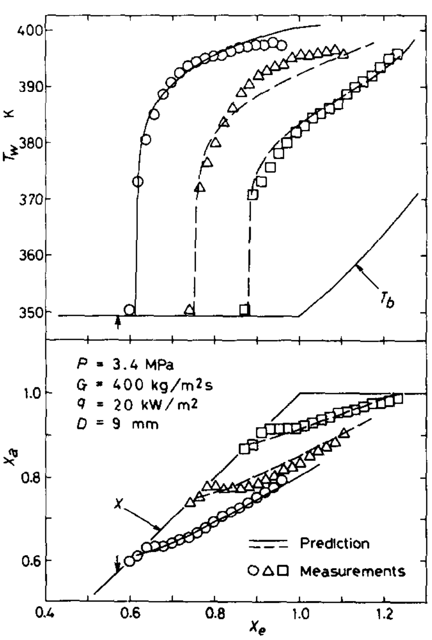

FIG. 4. Predicted and measured wall temperature and actual quality vs equilibrium quality.

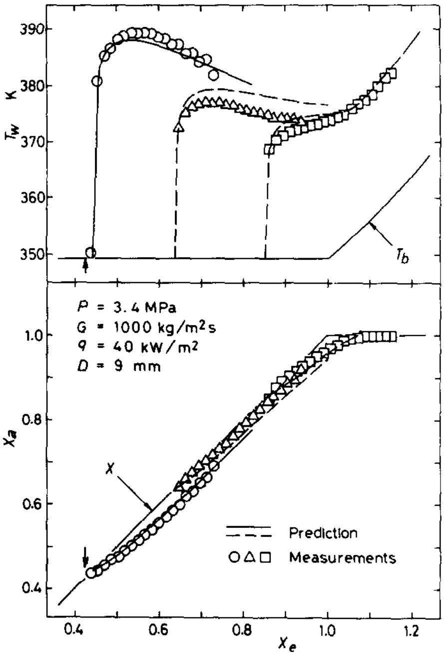

FIG. 5. Predicted and measured wall temperature and actual quality vs equilibrium quality.

6. CONCLUSIONS

The following results are obtained from the experiments and analyses on the post-dryout heat transfer to Freon 22 flowing upward in the uniformly heated vertical tube at high subcritical pressures.

1. None of correlations which have been proposed hitherto for the post-dryout heat transfer are applicable to the present case.
2. A conventional theoretical model is not able to reproduce satisfactorily the wall temperature for the present heat transfer.
3. A nondimensional parameter Kn which governs

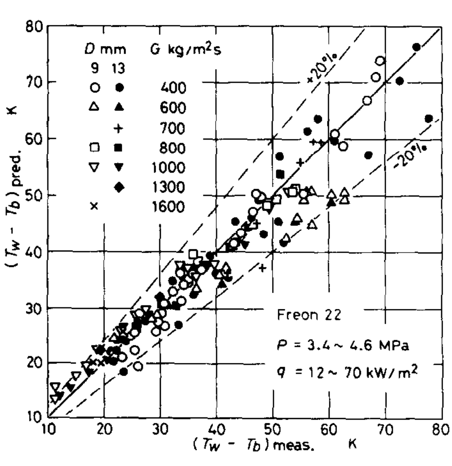

FIG. 6. Comparison of the predicted temperature differences between wall and bulk fluid with the measured values.

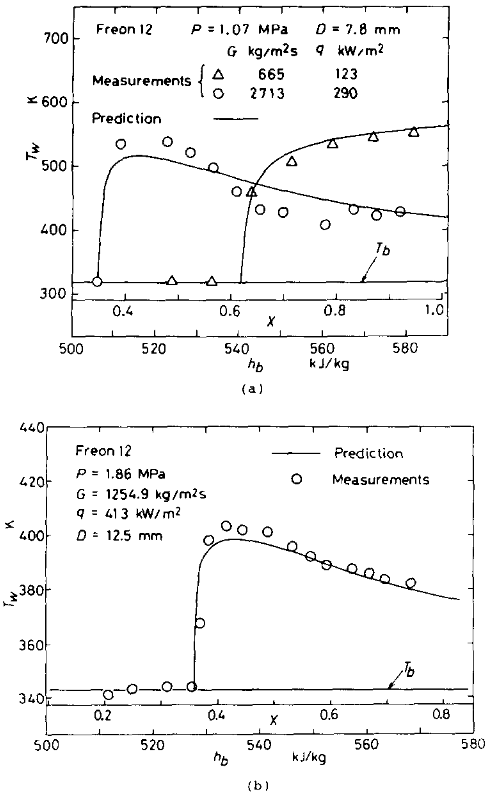

FIG. 7. Comparison of the predicted wall temperature with Groeneveld's [13] data (a) and Schnittger's [14] data (b).

the thermodynamic nonequilibrium of the two-phase fluid was introduced to a model for the post-dryout regime, and a correlation of *Kn* was developed. The proposed method by the use of this correlation successfully predicts the wall temperature for the post-dryout heat transfer to Freon at high subcritical pressures.

4. The present prediction method is possible to be applied to Freon also at pressures lower than those in the present study.

The heat transfer in the relatively high quality region was considered in the present study. The study of the heat transfer in the low quality or subcooled region, where the film boiling in inverted annular flow pattern is presumably predominant, is intended successively to clarify the heat transfer characteristics of Freon throughout the post-burnout region.

Acknowledgements—This work was supported in part by a Grant-in-Aid for Special Project Research of Energy No. 58045116 (1983) and No. 59045108 (1984) from the Ministry of Education, Science and Culture of Japan.

REFERENCES

1. K. Nishikawa, S. Yoshida, A. Yamada and M. Ohno, Experimental investigation of critical heat flux in forced convection boiling of Freon in a tube at high subcritical pressure, *Proc. 7th Int. Heat Transfer Conference*, Munich, Vol. 4, pp. 321–326 (1982).
2. S. Yoshida, K. Nishikawa, H. Mori, A. Yamada and M. Ohno, Heat transfer to Freon near the critical pressure flowing in tubes (2nd report, critical heat flux at inlet conditions of vapor–liquid mixture) (in Japanese), *Trans. Japan Soc. mech. Engrs* **51**, 563–571 (1985).
3. K. Nishikawa, S. Yoshida, H. Mori and H. Takamatsu, An experiment on the heat transfer characteristics in the post-burnout region at high subcritical pressures, *Nucl. Engng Des.* **74**, 233–239 (1982).
4. D. C. Groeneveld and G. G. J. Delorme, Prediction of thermal non-equilibrium in the post-dryout regime, *Nucl. Engng Des.* **36**, 17–26 (1976).
5. D. N. Plummer, O. C. Iloeje, W. M. Rohsenow, P. Griffith and E. Ganic, Post critical heat transfer to flowing liquid in a vertical tube, MIT Department of Mechanical Engineering Report No. 72718-91 (1974).
6. P. Saha, A nonequilibrium heat transfer model for dispersed droplet post-dryout regime, *Int. J. Heat Mass Transfer* **23**, 483–492 (1980).
7. G. L. Yoder, Jr. and W. M. Rohsenow, A solution for dispersed flow heat transfer using equilibrium fluid conditions, *J. Heat Transfer* **105**, 10–17 (1983).
8. A. W. Bennett, G. F. Hewitt, H. A. Kearsey and R. K. F. Keys, Heat transfer to steam–water mixtures flowing in uniformly heated tubes in which the critical heat flux has been exceeded, UKAEA Research Group Report AERE-R5373 (1967).
9. R. P. Forslund and W. M. Rohsenow, Dispersed flow film boiling, *J. Heat Transfer* **90**, 399–407 (1968).
10. Y. Koizumi, T. Ueda and H. Tanaka, Post dryout heat transfer to R-113 upward flow in a vertical tube, *Int. J. Heat Mass Transfer* **22**, 669–678 (1979).
11. T. Ueda, Entrainment rate and size of entrained droplets in annular two-phase flow, *Bull. JSME* **22**, 1258–1265 (1979).
12. M. Cumo, G. E. Farello, G. Ferrari and G. Palazzi, On two-phase highly dispersed flows, *J. Heat Transfer* **96**, 496–503 (1974).
13. D. C. Groeneveld, The thermal behavior of a heated surface at and beyond dryout, AECL-4309 (1972).
14. R. B. Schnittger, Untersuchungen zum Wärmeübergang bei vertikalen und horizontalen Rohrströmungen in Post-Dryout-Bereich. Dissertation, Universität Hannover, F.R.G. (1982).
15. P. Eisenklam, S. A. Arunachalam and J. A. Weston, Evaporation rates and drag resistance of burning drops, *Proc. 11th Symposium on Combustion*, pp. 715–728 (1967).
16. R. B. Bird, W. E. Stewart and E. N. Lightfoot, *Transport Phenomena*, p. 192. Wiley, New York (1960).
17. M. C. Yuen and L. W. Chen, Heat transfer measurements of evaporating liquid droplets, *Int. J. Heat Mass Transfer* **21**, 537–542 (1978).

APPENDIX: THEORETICAL MODEL

Energy equation for the two-phase dispersed flow:

$$\frac{dx_a}{dx_e} = \frac{q_d}{q} \tag{4}$$

where

$$q_d = \frac{\pi}{4} D_d^2 D N \alpha_d (T_v - T_s) \tag{A1}$$

and assuming no breakup of liquid droplets

$$N = \frac{6G(1-x_a)}{\pi D_d^3 \rho_l u_d}. \tag{A2}$$

Energy equation for a liquid droplet:

$$\frac{dD_d}{dx_e} = -\frac{GD\alpha_d}{2q\rho_l u_d}(T_v - T_s). \tag{A3}$$

Equation of motion for a liquid droplet:

$$\frac{du_d}{dx_e} = \frac{GDh_{fg}}{4q}\left[\frac{3}{4}\frac{C_D\rho_v(u_v-u_d)^2}{\rho_l u_d D_d} - \frac{(\rho_l-\rho_v)g}{\rho_l u_d}\right] \tag{A4}$$

where from refs. [15, 16]

$$C_D = \frac{C_{D0}}{1+B} \tag{A5}$$

$$C_{D0} = \begin{cases} 24Re_d^{-1}; Re_d \leqslant 2 \\ 18.5Re_d^{-0.6}; 2 < Re_d \leqslant 5\times10^2 \\ 0.44; 5\times10^2 < Re_d < 2\times10^5 \end{cases} \tag{A6}$$

$$B = \frac{h_v - h_{vs}}{h_{fg}} \tag{A7}$$

$$Re_d = \frac{\rho_v(u_v-u_d)D_d}{\mu_v} \tag{A8}$$

and

$$u_v = \frac{Gx_a u_d \rho_l}{[\rho_l u_d - G(1-x_a)]\rho_v}. \tag{A9}$$

Heat transfer coefficient from the vapor to the liquid droplet [17]:

$$\frac{\alpha_d D_d}{\lambda_v} = \frac{1}{1+B}(2+0.6Re_d^{1/2}Pr_v^{1/3}). \tag{A10}$$

The actual quality x_a and the vapor temperature T_v are calculated by solving equations (3), (4), (A3) and (A4) simultaneously and numerically for given boundary conditions:

$$\left.\begin{aligned} \text{at}\quad & x_e = x_c; \\ & x_a = x_c \\ & D_d = D_{dc} \\ & u_d = u_{dc} = G\left(\frac{x_c}{\rho_{vs}S_c} + \frac{1-x_c}{\rho_l}\right). \end{aligned}\right\} \tag{A11}$$

Substituting the values of x_a and T_v thus obtained into equations (1) and (2), the wall temperature T_w is calculated for a prescribed wall heat flux.

TRANSFERT THERMIQUE APRES ASSECHEMENT DE FREON DANS UN TUBE VERTICAL A DES PRESSIONS SOUS-CRITIQUES

Résumé—Des études de transfert thermique après assèchement sont conduites expérimentalement pour du Freon 22 qui s'élève dans un tube circulaire vertical à des pressions fortement sous-critiques (pression réduite entre 0,68 et 0,92). Un modèle théorique ne représente pas bien la température mesurée de la paroi. On introduit un paramètre addimensionnel *Kn* pour tenir compte du déséquilibre thermodynamique entre la vapeur et les gouttelettes de liquide. Une formule est donnée pour *Kn* et une méthode permet de calculer correctement la température de la paroi.

WÄRMEÜBERGANG IM POST-DRYOUT-BEREICH MIT FREON IM SENKRECHTEN ROHR BEI HOHEN UNTERKRITISCHEN DRÜCKEN

Zusammenfassung—Es wurden Untersuchungen zum Wärmeübergang im Post-Dryout-Bereich durchgeführt, die auf experimentellen Daten des Wärmeübergangs von Freon 22 beruhen, welches in einem senkrechten Rohr bei hohen unterkritischen Drücken (normierte Drücke von 0,68 bis 0,92) aufwärts strömt. Ein konventionelles theoretisches Modell versagte zum Teil bei der Reproduktion der gemessenen Wandtemperaturen. Ein dimensionsloser Parameter Kn wurde in ein Modell für den Post-Dryout-Bereich eingeführt, um das thermodynamische Nichtgleichgewicht zwischen dem Dampf und den Flüssigkeitstropfen zu berücksichtigen. Es wurde eine Korrelation für Kn entwickelt. Eine Methode, welche diese Korrelation verwendet, war in der Vorausberechnung der Wandtemperatur erfolgreich.

ЗАКРИТИЧЕСКИЙ ТЕПЛОПЕРЕНОС К ФРЕОНУ В ВЕРТИКАЛЬНОЙ ТРУБЕ ПРИ ДАВЛЕНИЯХ, ЗНАЧИТЕЛЬНО МЕНЬШИХ КРИТИЧЕСКОГО

Аннотация—Изучен закритический теплообмен на основе экспериментальных данных по теплопереносу к фреону 22, движущемуся вверх в вертикальной круглой трубе при давлениях, значительно меньших критического (приведенное давление изменяется от 0,68 до 0,92). С помощью известной теоретической модели невозможно правильно рассчитать измеренную температуру стенки. Для учета термодинамической равновесности между паром и каплями жидкости в модель закритического режима введен безразмерный параметр *Kn*. Модифицированный таким образом метод успешно использован для расчета температуры стенки.